Linear Programming Based Design and Analysis of Battery Pack Balancing Topologies

Ran Gu*, Pawel Malysz+, Matthias Preindl*, Hong Yang+, Ali Emadi*
*Electrical and Computer Engineering Department, McMaster University
McMaster Institute for Automotive Research and Technology (MacAUTO)
Hamilton, Ontario, Canada
+Fiat Chrysler Automobiles, Auburn Hills, Michigan, USA
E-mail: pawel.malysz@fcagroup.com

Abstract—**High voltage Li-ion battery packs are typically configured in a modular fashion. In this paper, the performance of different battery pack balancing topologies is analysed at both module and cell levels. Two-level balancing topologies, including cell-to-cell balancing at intra-module level and module-to-module balancing at inter-module level, are considered in the analysis. Topologies are comprised of combinations of line shunting, ring shunting, synchronous fly-back, multi-winding, and dissipative shunting. Aspects of battery pack balancing performance, such as minimum balancing time, minimum plug-in charge time, and minimal energy loss in balancing are calculated using linear programming. Component counts of every balancing topology for the entire battery pack are also compared to assess circuit complexity.**

I. Introduction

As an energy source in electrified vehicles, the battery pack provides energy and power to the vehicle [1]. The operational voltage of the battery pack usually requires many cells to be connected in series to optimize power, efficiency and cost of the electrified powertrain. Cell to cell differences in capacity and impedance are common sources of imbalance in the battery pack. Cell imbalance can lead to incomplete use of pack energy and can accelerate cell aging/degradation.

There are many balancing methods developed to handle this problem [2]. Most approaches are actively controlled such that the battery management system must open/close switches and control other electronic components [3]. They can be further classified into dissipative balancing and redistributive balancing methods. Dissipative balancing is simple, but has high energy loss. A typical dissipative balancing method uses shunting resistors [4], [5]. Many redistributive balancing topologies have been proposed [4]–[12], these aim for higher energy efficiency through transfer of energy between cells. However, redistributive balancing methods typically have higher complexity and cost compared to dissipative balancing. Recently, Daowd et al. have proposed a pack-level balancing system using different redistributive balancing methods at the cell and module connection levels [13].

The balancing topology should operate in an optimal manner to achieve different balancing control objectives. Balancing control objectives can be classified into voltage based, state of charge (SOC) based, and capacity based [14]. Einhor et al. [11] demonstrated through simulation and experimental testing that SOC and capacity based methods are more effective than a voltage based approach. The SOC and capacity based balancing approaches require high-accuracy algorithms for SOC and capacity estimation to operate optimally.

The balancing control strategy and its algorithm also affect performance of the balancing system. Caspar and Hohmann proposed an on-line optimization based strategy that considered a non-linear cell model and inductive balancing circuits. The goal of their approach was to reduce energy loss during the balancing process, moreover a dynamic optimization algorithm was applied to find the optimal switching sequence and duty cycle. Fuzzy logic based control algorithms have also been proposed to adaptively control equalization currents [15], [16]. Recently, Najmabadi evaluated cell-to-cell and cell-to-pack based control approaches on a redistributive balancing prototype [17].

Analytical research on performance and optimal design of balancing circuits have also been recently performed. Narayanaswamy et al. [18] used multi-objective optimization for minimizing energy dissipation losses and installation volume. Switching and conduction losses of different electronic components were considered in the design optimization. Baronti et al. [7] developed generalized models of four redistributive balancing topologies to calculate the minimum energy loss and the balancing time. Performance of a balancing topology was analysed numerically using probability density function distributions of many initial cell state cases. Preindl et al. [6] proposed a linear programming based method to compute the worst case balancing time and energy loss among different balancing topologies. Symmetries and convexity properties of the topologies were exploited to make the method computationally tractable when determining worse cast performance given ranges of cell initial SOC states.

High voltage Li-ion battery packs are typically configured in a modular fashion where multiple cells are connected in series to form modules and multiple modules are connected in series to form the battery pack. Balancing is needed at both module and cell level, i.e. cells are balanced within a module, and modules balanced at the pack level. Performance of the battery pack is influenced by the balancing circuit design and the battery size factor (BSF), the latter refers to the battery pack configuration such as the number of cells in series inside

978-1-4673-6741-7/15/$31.00 ©2015 IEEE

a module and the number of modules in series that form the battery pack. Balancing time, plug-in charge time, and energy loss of five balancing topologies, including line shunting, ring shunting, synchronous flyback, multi-winding, and dissipative shunting are studied at both module and pack levels. A total of 25 combinations of different two-level balancing topologies are evaluated in this paper The linear programming approach presented in [6] is extended to consider a modular battery pack design and mixed combinations of dissipative/redistributive balancing. Components counts of the two-level topology combinations are also presented. The performance is benchmarked against conventional dissipative balancing.

The rest of the paper is organized as follows. The linear programming based analysis method is shown in Section II. Section III presents four redistributive balancing topologies that are used at both cell balancing and module balancing levels. In Section IV, pack-level analysis is presented. Conclusions and future work is highlighted in Section V.

II. Balancing Topology Analysis Method Based on Linear Programming

In this section, a linear programming based analysis method is presented. Equality constraints, inequality constraints, and the objective functions are presented. A more theoretical presentation of the basics of this approach are provided in [6]. The balancing algorithm is based on SOC, the stored charge in a cell at time τ can be expressed using Coulomb counting as

$$SOC(\tau) = SOC(0) + \frac{1}{Q}\int_0^{\tau} i(t)dt \tag{1}$$

where $SOC(0)$ is the initial SOC, Q is the total capacity in units Ah, and i is current through the cell. In a battery pack system, the current includes charging/discharging current of the pack and the balancing current into/from individual cells.

Many balancing circuits work with high frequency switching power electronics. In this paper, the analysis ignores cell electrochemical dynamics and focuses on average charge movement between cells to find the optimal average balancing commands including the selection of cells being balanced, balancing current amount and direction. The distributed charge in cell j during time τ is linearized to $i_{bj}\tau$ with unit Ah, where i_{bj} is the average balancing current of the j^{th} cell. The SOC of the cells and the balancing topology is represented in the form

$$\begin{bmatrix} SOC_1(\tau) \\ \vdots \\ SOC_n(\tau) \end{bmatrix} = \begin{bmatrix} SOC_1(0) \\ \vdots \\ SOC_n(0) \end{bmatrix} + \frac{1}{Q}\mathbf{T}\begin{bmatrix} i_{b1}\tau \\ \vdots \\ i_{bn}\tau \end{bmatrix} \tag{2}$$

where the topology matrix $\mathbf{T}$ represents the interconnection capabilities and modular design of the two-level battery pack balancing topology.

An equality constraint is needed to represent a balanced system state at the terminal time τ. When all cells in a string are balanced, the SOC of all the cells satisfy

$$SOC_1 = SOC_2 = \ldots = SOC_n = \frac{1}{n}\sum_1^n SOC_i \tag{3}$$

This can be expressed as

$$\mathbf{L}\mathbf{x}(\tau) = 0 \tag{4}$$

where

$$\mathbf{x}(\tau) = [SOC_1(\tau)\ \ SOC_2(\tau)\ \ \ldots\ \ SOC_n(\tau)]^T \tag{5}$$

$$\mathbf{L} = \left(\mathbf{I} - \frac{1}{n}\mathbf{1}\cdot\mathbf{1}^T\right) \tag{6}$$

Considering the average balancing command

$$\mathbf{v} = \mathbf{u}\tau = [i_{b1}\tau\ \ i_{b2}\tau\ \ \ldots\ i_{bn}\tau]^T \tag{7}$$

and the initial cell SOC states $\mathbf{x}(0)$, the equality constraint becomes

$$\mathbf{L}\mathbf{x}(0) + \mathbf{L}\frac{1}{Q}\mathbf{T}\mathbf{v} = 0 \tag{8}$$

When considering minimum plug-in charge time, the equality constraint is modified to ensure that the SOC of each cell is 100% fully charged at time τ. This leads to a simplified equality constraint

$$\mathbf{x}(0) + \frac{1}{Q}\mathbf{T}\mathbf{v} = \mathbf{1} \tag{9}$$

Inequality constraints are needed to represent limits of balancing currents. This leads to the balancing current vector $\mathbf{u}$ to be subject to a constraint of the form $\mathbf{H}\mathbf{u} \leq \mathbf{k}$, multiplying both sides by the balancing time τ yields

$$[\mathbf{H}\ \ -\mathbf{k}]\begin{bmatrix} \mathbf{v} \\ \tau \end{bmatrix} \leq 0 \tag{10}$$

When considering energy dissipatation, it should be noted that the balancing current vector should also contain absolute values of the balancing current, i.e. $\mathbf{u} = [i_{b1}, i_{b2}, \ldots, i_{bn}, |i_{b1}|, |i_{b2}|, \ldots, |i_{bn}|]^T$ and $\mathbf{v} = [i_{b1}\tau, i_{b2}\tau, \ldots, i_{bn}\tau, |i_{b1}|\tau, |i_{b2}|\tau, \ldots, |i_{bn}|\tau]^T$. The vector $[\mathbf{v}\ \tau]^T$ becomes the vector that the linear programming optimization solver computes.

Two objective functions are possible, one related to balancing time, the other to energy dissipated. The solution to the formulated linear program provides the optimal balancing command for a topology considering different sets of initial conditions, e.g. varying spreads of cell SOC. To evaluate the worst-case performance of balancing time and energy dissipated of a topology more efficiently, an approach exploiting topology symmetries is used [6]. Instead of n^2 cases, this approach considers the following $n-1$ limiting extremes cases [6]

$$\mathbf{x}(0) = \left(\frac{SOC_{high} - SOC_{low}}{2}\right)\begin{bmatrix} \mathbf{1}_{n-k} \\ -\mathbf{1}_k \end{bmatrix} + \left(\frac{SOC_{high} + SOC_{low}}{2}\right), k = 1, \ldots, n-1 \tag{11}$$

The objective function for computing the worst-case balancing time or plug-in charge time is

$$\max_{k\in\{1,\ldots,n-1\}} \min \quad \tau \tag{12}$$

The objective function for computing the worst-case energy dissipated of a topology is

$$\max_{k\in\{1,\ldots,n-1\}} \min \quad \sum_{i=1}^{n} (1-\eta) \overbrace{\mathbf{v}_{n+i}}^{|i_{bi}|\tau} \tag{13}$$

where η is the link efficiency of the topology. In this paper, an efficiency of 90% is assumed.

III. Balancing Topologies

In this section, passive balancing and four inductor/transformer based topologies, depicted in Fig. 1, are considered. A topology matrix $\mathbf{T}$ is introduced for each case to describe the relation between balancing current and SOC. A linearized analysis is performed by simplifying the dynamic process of balancing to an average balancing current over the balancing time-interval from 0 to τ.

A. Dissipative shunting

Conventional passive balancing dissipates energy through a shunting resistor for each cell. The topology matrix is a negative diagonal matrix $\mathbf{T} = diag([-1 \cdots -1])$. When balancing, the magnitude of the balancing currents i_{bi} is assumed to be constant, its value can be approximated as the nominal cell voltage divided by the shunting resistance. For a more fair comparison the same maximum magnitude is used for passive and active balancing, however charging current are not allowed when dissipative shunting is used. The inequality constraints can easily be modified to enforce this [6].

B. Line shunting

Line shunting topology is shown in Fig. 1(a). In this topology, charge of neighboring cells are moved by a converter [8]. Therefore, n cells in series need n-1 converters. The topology matrix for line shunting is

$$\mathbf{T} = \begin{bmatrix} 1 & & & & \\ -1 & 1 & & & \\ & -1 & 1 & & \\ & & \ddots & \ddots & \\ & & & -1 & 1 \\ & & & & -1 \end{bmatrix}_{n\times(n-1)} \tag{14}$$

The balancing current is limited by the current limits $|i_{bi}| \leq i_{limit}$. This leads to the following inequality constraint

$$\overbrace{\begin{bmatrix} \mathbf{I}_{n\times n} & -\mathbf{I}_{n\times n} \\ -\mathbf{I}_{n\times n} & -\mathbf{I}_{n\times n} \\ \mathbf{0}_{n\times n} & \mathbf{I}_{n\times n} \\ \mathbf{0}_{n\times n} & -\mathbf{I}_{n\times n} \end{bmatrix}}^{\mathbf{H}} \overbrace{\begin{bmatrix} i_{b1} \\ \vdots \\ i_{bn} \\ |i_{b1}| \\ \vdots \\ |i_{bn}| \end{bmatrix}}^{\mathbf{u}} \leq \overbrace{\begin{bmatrix} \mathbf{0}_{n\times 1} \\ \mathbf{0}_{n\times 1} \\ i_{limit}\cdot \mathbf{1}_{n\times 1} \\ \mathbf{0}_{n\times 1} \end{bmatrix}}^{\mathbf{k}} \tag{15}$$

C. Ring shunting

The ring shunting topology is shown in Fig. 1(b). It is similar with line shunting, but the first cell and the last cell are connected by a fly-back converter [6]. The topology matrix is given by

$$\mathbf{T} = \begin{bmatrix} 1 & & & & -1 \\ -1 & 1 & & & \\ & -1 & 1 & & \\ & & \ddots & \ddots & \\ & & & -1 & 1 \end{bmatrix}_{n\times n} \tag{16}$$

The balancing current has the same limitation as with line shunting, so the matrix $\mathbf{H}$ and vector $\mathbf{k}$ are the same as with line shunting shown in (15).

D. Synchronous fly-back converter

Fig. 1(c) shows the circuit topology of synchronous fly-back converter based active balancing. Each cell in the string is connected with the entire module by an independent bidirectional synchronous fly-back converter [10]. The i^{th} cell is balanced by the secondary side current of the i^{th} fly-back converter i_{is} and the primary side current of all fly-back converters i_{ip}, where subscript $i \in [1, n]$. The cells SOC at terminal time τ is derived as

$$\begin{aligned} SOC_i(\tau) \quad &= \quad SOC_i(0) + \frac{1}{Q}\int_{t=0}^{\tau} i_{is}(t)dt \\ &\quad -\frac{1}{Q}\left(\int_{t=0}^{\tau} i_{1p}(t)dt + \ldots + \int_{t=0}^{\tau} i_{np}(t)dt\right) \end{aligned} \tag{17}$$

The relationship between average secondary side and primary side currents is given by $\mathbf{I}_s = n\mathbf{I}_p$. Therefore, the battery system in linear form is

$$\begin{bmatrix} SOC_1(\tau) \\ SOC_2(\tau) \\ \vdots \\ SOC_n(\tau) \end{bmatrix} = \begin{bmatrix} SOC_1(0) \\ SOC_2(0) \\ \vdots \\ SOC_n(0) \end{bmatrix} + \frac{1}{Q}\mathbf{T} \begin{bmatrix} i_{b1}\tau \\ i_{b2}\tau \\ \vdots \\ i_{bn}\tau \end{bmatrix} \tag{18}$$

where the topology matrix is

$$\mathbf{T} = \begin{bmatrix} 1-\frac{1}{n} & -\frac{1}{n} & \ldots & -\frac{1}{n} \\ -\frac{1}{n} & 1-\frac{1}{n} & \ldots & -\frac{1}{n} \\ \vdots & \vdots & \ddots & \vdots \\ -\frac{1}{n} & -\frac{1}{n} & \ldots & -1\frac{1}{n} \end{bmatrix} \tag{19}$$

Since the fly-back converters in the topology are independent, the balancing currents are also limited by (15).

E. Multi-winding transformer

Multi-winding transformer based topology is shown in Fig. 1(d). It should be emphasized that only one secondary side winding works in one cycle [9], [11], [12]. In one cycle, one cell is active and the other $n-1$ are inactive. The cells SOC are expressed by

$$SOC_i(k+1) \quad = \quad SOC_i(k) + \tfrac{1}{Q}i_{is}(t)dt - \tfrac{1}{Q}i_{ip}(t)dt \tag{20}$$

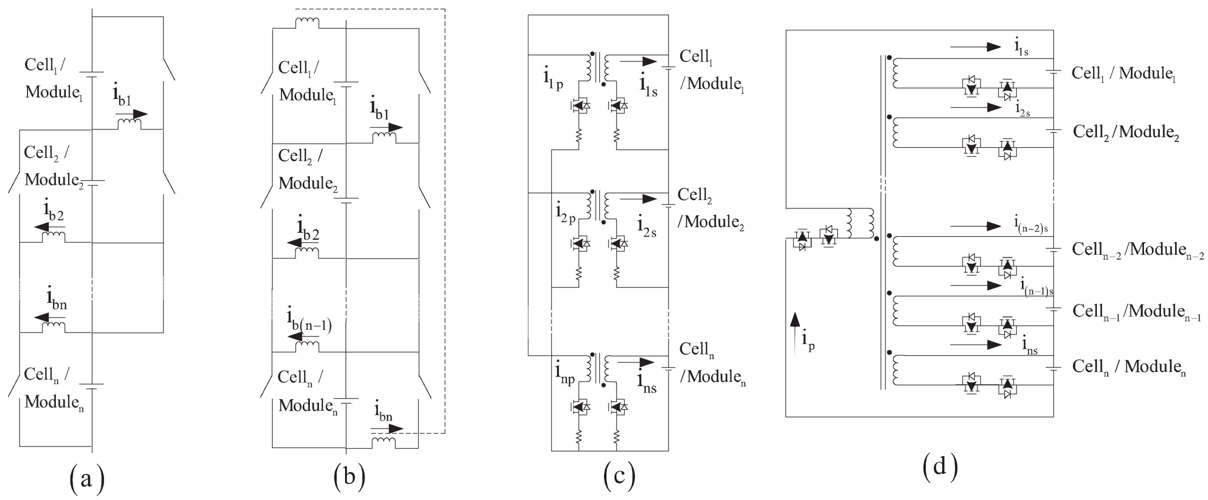

Fig. 1: Four actively controlled redistributive balancing topologies a) Line Shunting b) Ring Shunting c) Sychronous Fly-back Converter d) Multi-winding transformer. Note each topology design is assumed to balance a string of cells and/or a string of modules.

for one active winding, and

$$SOC_j(k+1) \quad = \quad SOC_j(k) - \tfrac{1}{Q} i_{jp}(t)dt \tag{21}$$

for n-1 inactive windings. Note $i \neq j$. Over a long time-scale τ, the state of charge of a cell can be expressed as

$$\begin{aligned} SOC_i(\tau) \quad &= \quad SOC_i(0) + \frac{1}{Q}\int_{t=0}^{\tau} i_{is}(t)dt \\ &-\frac{1}{Q}\left(\underbrace{\int_{t=0}^{\tau} i_p(t)dt + \ldots + \int_{t=0}^{\tau} i_p(t)dt}_{n}\right) \end{aligned} \tag{22}$$

The topology matrix of the multi-winding transformer is derived in the same form as the synchronous fly-back converter. However since there is only one active winding in one cycle, the balancing currents should be limited by additional constraints $|i_{bi}| \leq i_{limit}$ and $\sum_{i=1}^{n} |i_{bi}| \leq i_{limit}$. The overall inequality constraint is

$$\begin{bmatrix} \mathbf{I}_{n\times n} & -\mathbf{I}_{n\times n} \\ -\mathbf{I}_{n\times n} & -\mathbf{I}_{n\times n} \\ \mathbf{0}_{n\times n} & \mathbf{I}_{n\times n} \\ \mathbf{0}_{n\times n} & -\mathbf{I}_{n\times n} \\ \mathbf{0}_{1\times n} & \mathbf{1}_{1\times n} \end{bmatrix} \begin{bmatrix} i_{b1} \\ \vdots \\ i_{bn} \\ |i_{b1}| \\ \vdots \\ |i_{bn}| \end{bmatrix} \leq \begin{bmatrix} \mathbf{0}_{n\times 1} \\ \mathbf{0}_{n\times 1} \\ i_{limit}\cdot \mathbf{1}_{n\times 1} \\ \mathbf{0}_{n\times 1} \\ i_{limit} \end{bmatrix} \tag{23}$$

IV. Battery Pack Balancing Analysis

The overall topology of the battery pack structure, from cell to module and from module to pack, will affect the overall balancing performance. If a battery pack has 96 cells in series, e.g. Fig. 2, there are many ways to integrate multiple cells in a module and then integrate modules to form a pack. In this paper, four kinds of subdivisions are considered, these include 6x16, 8x12, 12x8 and 16x6 arrangements where the former is the number of modules and the latter is cells per module. The four redistributive topologies considered in this paper generate 16 combinations of pure redistributive balancing pack topologies. In addition, 8 mixed two-level dissipative/redistributive balancing topologies are also considered. One dissipative only balancing topology is used as a benchmark.

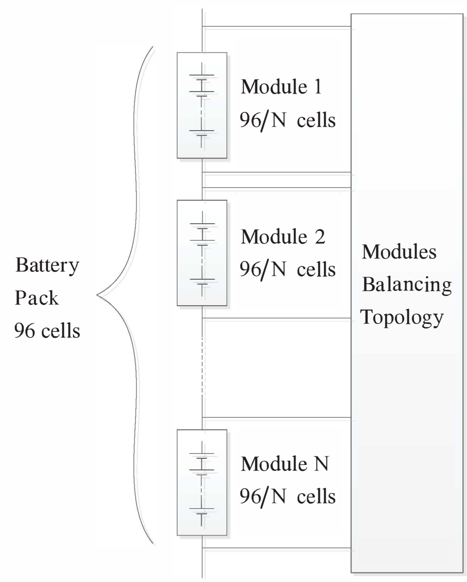

Fig. 2: Battery pack two level balancing topology. Each module employs a dissipative balancing circuit or one of the four redistributive circuits in Fig. 1.

To consider different battery pack architectures, the topology matrix for the battery pack needs to be modified to account for the two level structuring. Cell SOC balanced via two levels is given by

$$SOC(\tau) = SOC(0) + \frac{1}{Q}\int i_b^{module}(t)dt + \frac{1}{Q}\int i_b^{pack}(t)dt \tag{24}$$

The last two terms are controllable balancing currents in module level representing cell-to-cell balancing current and pack level representing module-to-module balancing current, respectively. If a 96 cell battery pack consists of m modules and each module contains n cell, the SOCs of the battery pack can be expressed as

$$\begin{bmatrix} SOC_1(\tau) \\ \vdots \\ SOC_{96}(\tau) \end{bmatrix} = \begin{bmatrix} SOC_1(0) \\ \vdots \\ SOC_{96}(0) \end{bmatrix} \tag{25}$$

$$+\frac{1}{Q}\begin{bmatrix} \mathbf{T}_m & & & \\ & \ddots & & \mathbf{T}_p \\ & & \mathbf{T}_m & \end{bmatrix} \begin{bmatrix} i_{b1}^{module}\tau \\ \vdots \\ i_{b96}^{module}\tau \\ i_{b1}^{pack}\tau \\ \vdots \\ i_{bm}^{pack}\tau \end{bmatrix}$$

where $\mathbf{T}_m$ and $\mathbf{T}_p$ represent topology matrices that are described in Section III. Subscript m and p denote module and pack levels, respectively. Topology matrices of these different complete pack balancing configurations are computed in Matlab script and solved using the linear program solver linprog [19]. Parameters of the battery pack are listed in Table I.

TABLE I: Parameters of battery pack

Number of cells	96
Number of modules	m
Number of cells per module	n
Maximum module/cell level balancing current	5A
Maximum initial SOC deviation	10%

A. Performance in idle mode

Performance of balancing topologies in idle mode, zero pack current, are analyzed in this section. Constraints (8) and (10) are employed. Figure 3a) and b) show the worst-case balancing time and the worst-case energy dissipation for different balancing combinations. Note that the x-axis represents one dissipative cell balancing topology, 16 redistributive balancing combinations, and 8 mixed balancing combinations. The capital letter before slash represents module level balancing topology and the capital letter after slash represents pack level balancing topology. D is dissipative shunting resistor as passive balancing topology, L is line shunting, R is ring shunting, F is synchronous fly-back, and M is multi-winding transformer. Four shaded bars denote 6, 8, 12, and 16 modules structures from dark blue to light blue.

From the results of these two plots, dissipative balancing topology has fast balancing time, but high energy loss. The multi-winding transformer topology leads to slow balancing time, because of only one channel working in one cycle. Combinations between ring shunting and synchronous fly-back converter have nice performance from these two aspects. As for the mixed balancing topologies, F/D configurations can provide fast balancing time. Considering energy loss, D/F and D/M topologies with 16 modules outperform other mixed

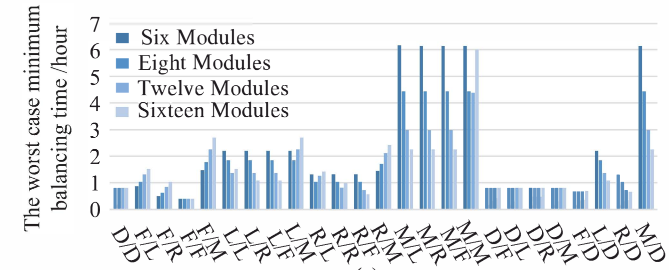

(a)

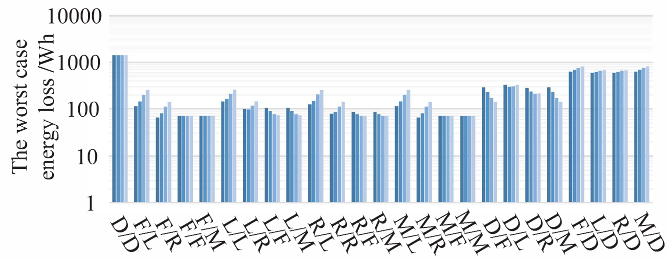

(b)

Fig. 3: Idle-mode performance analysis a) The worst-case minimum balancing time b) The worst-case minimum energy loss.

configurations. The shortest balancing time is 0.4 hour from combination of F/F. The lowest energy loss is 66Wh from combination F/R with six modules.

B. Performance in plug-in charge mode

The effect of balancing topology on the plug-in charge process is described here. It is assumed the battery pack is balanced at or before its fully charged state. A constant current $\frac{1}{4}$C mode pack charging scheme is assumed. These assumptions ensure feasibility of the combined charging and balancing process in terms of the simplified linear programming based analysis. The constraints employed are (9) and (10).

A subset of 16 two-level redistributive topologies are considered. The performance of 15 redistributive-balancing enabled topologies are compared with the dissipative balancing topology, results are shown in Fig. 4. The results depicted in Fig. 4a) indicates the redistributive only balancing topologies can slightly shorten the worst case charging time. This arises since the most energy is lost during the charging process as depicted in Fig. 4. Redistributive balancing enabled topologies can recover this energy to charge other cells.

C. Component counts

Major components needed for the balancing topologies are summarized in Table II. Circuits containing dissipative balancing at the cell or module level use fewer components.

V. Conclusions

From the above analysis, overall battery pack balancing topologies can be evaluated considering balancing time, energy loss, effect on plug-in charge and component counts. Five top performing two-level balancing topologies are compared,

TABLE II: Component Counts

	Number of switches	Number of sensor resistors	Number of inductors/ transformers
F/L	$2n \cdot m + 2(m-1)$	$2n \cdot m + (m-1)$	$m-1$ indcutors $n \cdot m$ 2-winding transformers
F/R	$2n \cdot m + 2m$	$2n \cdot m + m$	$m-1$ indcutors $n \cdot m + 1$ 2-winding transformers
F/F	$2n \cdot m + 2m$	$2n \cdot m + 2m$	$n \cdot m + m$ 2-winding transformers
F/M	$2n \cdot m + 2(m+1)$	$2n \cdot m + m$	$n \cdot m$ 2-winding transformers 1 m-winding transformer
L/L	$2(n-1) \cdot m + 2(m-1)$	$(n-1) \cdot m + (m-1)$	$(n-1) \cdot m + m - 1$ inductors
L/R	$2(n-1) \cdot m + 2m$	$(n-1) \cdot m + m$	$(n-1) \cdot m + m - 1$ inductors 1 2-winding transformer
L/F	$2(n-1) \cdot m + 2m$	$(n-1) \cdot m + 2m$	$(n-1) \cdot m$ inductors m 2-winding transformers
L/M	$2(n-1) \cdot m + 2(m+1)$	$(n-1) \cdot m + 1$	$(n-1) \cdot m$ inductors 1 m-winding transformer
R/L	$2n \cdot m + 2(m-1)$	$n \cdot m + (m-1)$	$(n-1) \cdot m + m - 1$ inductors m 2 winding-transformers
R/R	$2n \cdot m + 2m$	$n \cdot m + m$	$(n-1) \cdot m + m - 1$ inductors $m + 1$ 2 winding-transformers
R/F	$2n \cdot m + 2m$	$n \cdot m + 2m$	$(n-1) \cdot m$ inductors $2m$ 2-winding transformers
R/M	$2n \cdot m + 2(m+1)$	$n \cdot m + 1$	$(n-1) \cdot m$ indcutors m 2-winding transformers 1 m-winding transformer
M/L	$2(n-1) \cdot m + 2(m-1)$	$m + m - 1$	$m-1$ inductors m n-winding transformers
M/R	$2(n-1) \cdot m + 2m$	$m + m$	$m-1$ inductors 1 2-winding transformer m n-winding transformers
M/F	$2(n-1) \cdot m + 2m$	$m + 2m$	m 2-winding transformers m n-winding transformers
M/M	$2(n-1) \cdot m + 2(m+1)$	$m + 1$	1 m-winding transformer m n-winding transformers
D/F	$n \cdot m + 2m$	$n \cdot m + 2m$	m 2-winding transformers
D/L	$n \cdot m + 2(m-1)$	$n \cdot m + (m-1)$	$m-1$ inductors
D/R	$n \cdot m + 2m$	$n \cdot m + m$	$m-1$ inductors m n-winding transformers
D/M	$n \cdot m + 2(m+1)$	$n \cdot m + 1$	1 m-winding transformer
F/D	$2n \cdot m + m$	$2n \cdot m + n \cdot m$	$n \cdot m$ 2-winding transformers
L/D	$2(n-1)m + m$	$(n-1)m + n \cdot m$	(n-1)m inductors
R/D	$2n \cdot m + m$	$2n \cdot m$	$(n-1)m$ inductors m 2-winding transformers
M/D	$2(n+1)m + m$	$m + n \cdot m$	m n-winding transformers

two are pure redistributive-only balancing topologies, two are mixed balancing topologies, and the remaining is pure dissipative-only balancing topology. They are compared graphically in a spider-chart as shown in Fig. 5. In the spider chart, the scoring is from 0 in the center to 1 at the edge to represent bad to good comparative performance. Balancing time and energy loss in two modes of F/F with 6 modules and F/R with 6 modules outperform others. Compared with other mixed topologies, F/D with 6 modules has the fastest balancing time. The passive balancing topology and D/F with 16 modules need less components compared to others.

A linear programming based balancing topology analysis method is presented and applied to the design of a complete battery pack balancing topology. A two-level modular design approach is considered in the analysis. Performances of different battery pack structures and balancing topologies are compared. The method is applicable to other balancing topologies with controllable current.

ACKNOWLEDGEMENTS

This research was undertaken thanks to funding and support from the Canada Excellence Research Chairs (CERC) program, National Science and Engineering Research council of Canada (NSERC) Automotive Partnership Canada (APC), and Fiat Chrysler Automobiles.

REFERENCES

[1] A. Emadi, "Transportation 2.0," *Power and Energy Magazine, IEEE*, vol. 9, no. 4, pp. 18–29, 2011.

[2] P. P. Malysz, L. Gauchia, and H. H. Yang, "Fundamentals of electric energy storage systems," *Advanced Electric Drive Vehicles*, pp. 237–281, 2014.

[3] J. Cao and A. Emadi, "Batteries need electronics," *Industrial Electronics Magazine, IEEE*, vol. 5, no. 1, pp. 27–35, 2011.

[4] J. Cao, N. Schofield, and A. Emadi, "Battery balancing methods: A comprehensive review," in *Vehicle Power and Propulsion Conference, 2008. VPPC '08. IEEE*, pp. 1–6, IEEE, 2008.

[5] M. Daowd, N. Omar, P. Van Den Bossche, and J. Van Mierlo, "Passive and active battery balancing comparison based on matlab simulation," in *Vehicle Power and Propulsion Conference (VPPC), 2011 IEEE*, pp. 1–7, IEEE, 2011.

[6] M. Preindl, C. Danielson, and F. Borrelli, "Performance evaluation of battery balancing hardware," in *Control Conference (ECC), 2013 European*, pp. 4065–4070, IEEE, 2013.

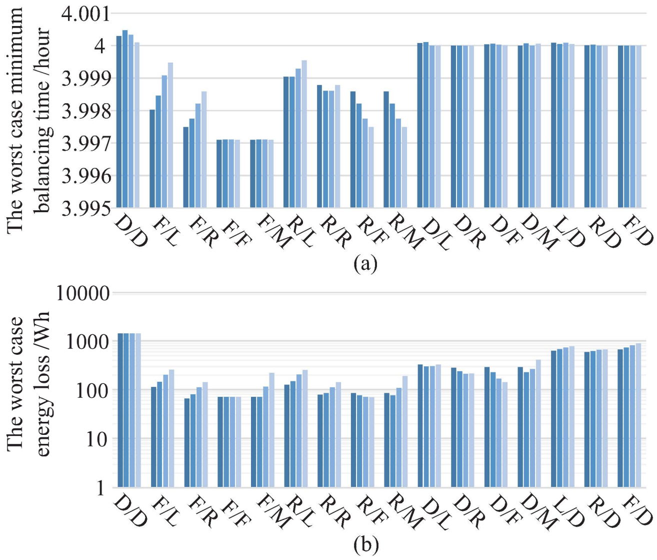

Fig. 4: Plug-in charge mode performance analysis a) The worst-case minimum balancing time b) The worst-case minimum energy loss.

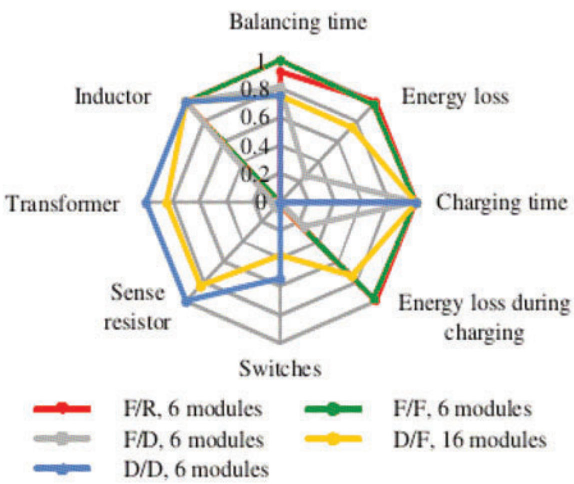

Fig. 5: Comparison of top performing designs.

[7] F. Baronti, R. Roncella, and R. Saletti, "Performance comparison of active balancing techniques for lithium-ion batteries," *Jounrnal of Power Sources*, vol. 267, pp. 603–609, Dec 2014.

[8] K. Nishijima, H. Sakamoto, and K. Harada, "A pwm controlled simple and high performance battery balancing system," in *Power Electronics Specialists Conference, 2000. PESC 00. 2000 IEEE 31st Annual (Volume:1)*, (Galway), pp. 517–520, IEEE, Jun 2000.

[9] C. Bonfiglio and W. Roessler, "A cost optimized battery management system with active cell balancing for lithium ion battery stacks," in *Vehicle Power and Propulsion Conference, 2009. VPPC '09. IEEE*, pp. 304–309, IEEE, 2009.

[10] Linear Technology, *LTC3300-1 - High Efficiency Bidirectional Multicell Battery Balancer.*

[11] M. Einhorn, W. Roessler, and J. Fleig, "Improved performance of serially connected li-ion batteries with active cell balancing in electric vehicles," *Vehicular Technology*, vol. 60, no. 6, pp. 2448–2457, 2011.

[12] J. Yun, T. Yeo, and J. Park, "High efficiency active cell balancing circuit with soft-switching technique for series-connected battery string," in *Applied Power Electronics Conference and Exposition (APEC)*, pp. 3301–3304, IEEE, 2013.

[13] M. Daowd, M. Antoine, N. Omar, P. Lataire, P. V. D. Bossche, and J. V. Mierlo, "Battery management system-balancing modularization based on a single switched capacitor and bi-directional dc/dc converter with the auxiliary battery," *Energies*, vol. 7, pp. 2897–2937, Dec 2014.

[14] Y. Barsukov and J. Qian, *Battery Power Management For Portable Devices*. Artech House., 2013.

[15] Y.-S. Lee and M.-W. Cheng, "Intelligent control battery equalization for series connected lithium-ion battery strings," *Industrial Electronics, IEEE Transactions on*, vol. 52, no. 5, pp. 1297–1307, 2005.

[16] J. Yan, Z. Cheng, G. Xu, H. Qian, and Y. Xu, "Fuzzy control for battery equalization based on state of charge," in *Vehicular Technology Conference Fall (VTC 2010-Fall), 2010 IEEE 72nd*, pp. 1–7, IEEE, 2010.

[17] A. Najmabadi, "Evaluation of active balancing algorithms and an improved method for a deployed active battery balancer as well as physical implementation," 2013.

[18] S. Narayanaswamy, S. Steinhoust, M. Lukasiewycz, M. Kauer, and S. Chakraborty, "Optimal dimensioning of active cell balancing architectures," in *Design, Automation and Test in Europe Conference and Exhibition (DATE)*, (Dresden), pp. 1–6, IEEE, Mar 2014.

[19] The MathWorks, Inc., *Linear Programming Solver*, 1998. MATLAB R2012b.